ELSEVIER

Contents lists available at ScienceDirect

# Fluid Phase Equilibria

journal homepage: www.sciencedirect.com/journal/fluid-phase-equilibria





# Differential equations for fluid phase equilibria: Isothermal-isobaric case

Ulrich K. Deiters

Institute of Light and Matter, University of Cologne, Greinstr. 4-6, D-50939 Köln, Germany

### ARTICLE INFO

Keywords:
Phase equilibrium
Gibbs triangle diagram
Ternary mixture
Differential equation
Isochoric thermodynamics

### ABSTRACT

Differential equations for two-phase equilibria under isothermal–isobaric conditions are derived. These equations can be used in connection with arbitrary equations of state (Helmholtz energy models) for fluid mixtures to compute phase envelopes. In contrast to conventional computation methods, which solve the (nonlinear) algebraic equations describing phase equilibrium by means of iterative methods and which often suffer from convergence problems, the differential equations merely have to be integrated, but not solved. Convergence problems are thus avoided. The computation of phase envelopes from differential equations is rapid, reliable, and advantageous in connection with complicated equations of state.

### 1. Introduction

Nowadays the calculation of phase equilibria of mixtures from equations of state is usually accomplished by solving a system of algebraic equations representing the thermodynamic equilibrium conditions. We mention here – on behalf of many others – the pioneering work of Michelsen [1], who already in 1980 proposed a method for computing isoplethic phase envelopes of multicomponent mixtures based on such algebraic equations. These equations are nonlinear; the solutions have to be found numerically by means of iteration methods, and convergence is not certain—particularly not if there are many components or if the underlying equation of state is very complicated.

This disadvantage is aggravated if the equation of state can return unphysical results for certain density–temperature combinations. A modern example is the GERG model [2], which makes it possible to calculate thermodynamic properties of mixtures with impressive accuracy. Unfortunately, a root finder algorithm that, on its path to the solution, accidentally runs into a problematic region is easily "derailed".

An alternative is the formulation of the equilibrium conditions as a system of differential equations. To obtain the phase envelopes, these equations have to be integrated, not solved; convergence problems are thus avoided.

An example of such differential equations are the Gibbs–Konowalow equations of 1881 [3] (originally for binary mixtures only; an extension to multicomponent mixtures can be found in [4]). These equations, however, are cumbersome to use with equations of state, as they have the pressure as an independent variable.

Differential equations that are particularly suited for use with equations of state have been proposed some years ago for isothermal as well as isobaric phase envelopes [5], for isopleths [6], and for critical curves [7], and their application to the construction of phase diagrams

has been demonstrated [8,9].

The differential equations published so far, however, do not cover the case of isothermal–isobaric phase envelopes for ternary and higher mixtures. Such phase envelopes are needed, for instance, to construct Gibbs triangle diagrams. This is the topic of this work.

## 2. Algorithm

### 2.1. Derivation

In the "isochoric thermodynamics" [10,11] formulation the central thermodynamic potential is the Helmholtz energy density,

$$\Psi(\vec{\rho}, T) = \frac{A(\vec{\rho}, T)}{V},\tag{1}$$

where  $\vec{\rho}$  is the vector of the concentrations or molar densities,

$$\vec{\rho} = \begin{pmatrix} \rho_1 \\ \vdots \\ \rho_N \end{pmatrix} \text{ with } \rho_i = x_i \rho = \frac{x_i}{V_{\text{m}}}$$
 (2)

 $(x_i$ : mole fraction of component i,  $V_m$ : molar volume).

The chemical potentials and the pressure are obtained from  $\Psi$  as

$$\vec{\mu} = \nabla \Psi$$

$$p = -\Psi + \vec{\mu} \cdot \vec{\rho},$$
(3)

where the differentiations are with respect to the concentrations  $\rho_i$ . The "·" denotes the scalar product. The total differentials of these properties

E-mail address: ulrich.deiters@uni-koeln.de.

are (cf. [5], Eqs. (18) and (20))

$$d\vec{\mu} = \boldsymbol{\Psi} \, d\vec{\rho} + \left(\frac{\partial \vec{\mu}}{\partial T}\right) \, dT$$

$$dp = (\boldsymbol{\Psi}\vec{\rho}) \cdot d\vec{\rho} + \left(\frac{\partial p}{\partial T}\right) \, dT.$$
(4)

Here  $\Psi$  stands for the Hessian matrix of  $\Psi$ ,

$$\Psi = \begin{pmatrix} \Psi_{11} & \dots & \Psi_{1N} \\ \vdots & \ddots & \vdots \\ \Psi_{N1} & \dots & \Psi_{NN} \end{pmatrix} \text{ with } \Psi_{ij} = \left( \frac{\partial^2 \Psi}{\partial \rho_i \, \partial \rho_j} \right). \tag{5}$$

 $\Psi$  is symmetric and, for stable phases, positive definite.

 $\mathrm{d}T$  and  $\mathrm{d}p$  are zero for isothermal-isobaric cases, hence the total differential of the pressure reduces to

$$dp = (\boldsymbol{\Psi}^{\chi} \vec{\rho}^{\chi}) \cdot d\vec{\rho}^{\chi} = 0, \tag{6}$$

where  $\chi=',''$  denotes the coexisting phases. Moreover, along the phase boundary we have  $\mathrm{d}\vec{\mu}''=\mathrm{d}\vec{\mu}',$ 

$$\Psi' \,\mathrm{d}\vec{\rho}' = \Psi'' \,\mathrm{d}\vec{\rho}''. \tag{7}$$

Multiplication with  $\vec{\rho}''$  (this is allowed for symmetric matrices) yields

$$(\boldsymbol{\Psi}'\vec{\rho}'')\cdot d\vec{\rho}' = (\boldsymbol{\Psi}''\vec{\rho}'')\cdot d\vec{\rho}'' \tag{8}$$

and, because of Eq. (6),

$$(\boldsymbol{\Psi}'\vec{\rho}'')\cdot d\vec{\rho}' = 0. \tag{9}$$

One way to proceed from here is making one mole fraction,  $x'_k$ , the marching variable. Dividing Eqs. (6) and (9) by  $dx'_k$  gives

$$(\boldsymbol{\Psi}'\vec{\rho}'')\cdot\vec{s}'=0\tag{10}$$

$$(\boldsymbol{\Psi}'\vec{\rho}')\cdot\vec{s}'=0,\tag{11}$$

where we have defined the "slope vector"

$$\vec{s}^{\,\chi} \equiv \frac{d\vec{\rho}^{\,\chi}}{dx_{\prime}'} \, . \tag{12}$$

The subscript " $\sigma$ " indicates that the derivatives are calculated along the phase envelopes, i.e., at saturation.

We note that

$$s'_{k} = \frac{\mathrm{d}\rho'_{k}}{\mathrm{d}x'_{k}}\bigg|_{\sigma} = \frac{\mathrm{d}(x'_{k}\rho')}{\mathrm{d}x'_{k}}\bigg|_{\sigma} = \rho' + x'_{k} \frac{\mathrm{d}\rho'}{\mathrm{d}x'_{k}}\bigg|_{\sigma} = \rho' + x'_{k} \sum_{i=1}^{N} \frac{\mathrm{d}\rho'_{i}}{\mathrm{d}x'_{k}}\bigg|_{\sigma} = \rho' + x'_{k} \sum_{i=1}^{N} s'_{i},$$
(12)

which after rearrangement yields

$$(1 - x'_k)s'_k - x'_k \sum_{i=1}^{n} s'_i = \rho'$$
 (14)

or, using vector notation,

$$\begin{pmatrix}
-x'_k \\
\vdots \\
-x'_k \\
1-x'_k \\
-x'_k \\
\vdots \\
-x'_k
\end{pmatrix} \cdot \begin{pmatrix}
s'_1 \\
\vdots \\
s'_{k-1} \\
s'_k \\
s'_{k+1} \\
\vdots \\
s'_N
\end{pmatrix} = \rho'.$$
(15)

According to Gibbs' phase rule 2-phase a N-component mixture at constant pressure and temperature has got N-2 thermodynamic degrees of freedom. For mixtures of four or more components it is necessary to specify N-3 constraints, e.g., that some mole fractions or some mole fraction ratios are kept constant. Ways to set up constraint equations have been described elsewhere [5].

Combining Eqs. (10), (11), and (15), and – for N > 3 – the constraint equations results in a system of linear equations for the derivatives  $s'_i$ ,

$$\begin{pmatrix} \vec{\Psi}'_{1} \cdot \vec{\rho}'' & \dots & \vec{\Psi}'_{k-1} \cdot \vec{\rho}'' & \vec{\Psi}'_{k} \cdot \vec{\rho}'' & \vec{\Psi}'_{k+1} \cdot \vec{\rho}'' & \dots & \vec{\Psi}'_{N} \cdot \vec{\rho}'' \\ \vec{\Psi}'_{1} \cdot \vec{\rho}' & \dots & \vec{\Psi}'_{k-1} \cdot \vec{\rho}' & \vec{\Psi}'_{k} \cdot \vec{\rho}' & \vec{\Psi}'_{k+1} \cdot \vec{\rho}' & \dots & \vec{\Psi}'_{N} \cdot \vec{\rho}' \\ -x'_{k} & \dots & -x'_{k} & 1 - x'_{k} & -x'_{k} & \dots & -x'_{k} \\ a_{l1} & \dots & a_{l,k-1} & a_{lk} & a_{l,k+1} & \dots & a_{lN} \\ \vdots & & \vdots & & \vdots & & \vdots \end{pmatrix}$$

$$\vdots \qquad \vdots \qquad \vdots \qquad \vdots \qquad \vdots \qquad \vdots$$

$$vith  $l = 1, \dots, N - 3.$  (16)$$

Here we have made use of the definition of the matrix-vector product,

$$\Psi'\vec{\rho}^{\chi} \equiv \begin{pmatrix} \vec{\Psi}_{1}' \cdot \vec{\rho}^{\chi} \\ \vdots \\ \vec{\Psi}_{N}' \cdot \vec{\rho}^{\chi} \end{pmatrix}, \tag{17}$$

where  $\vec{\Psi}'_{k}$  denotes the *k*th row vector of  $\Psi'$ .

Inserting Eq. (4) into the condition of equal  $d\vec{\mu}$  gives

$$\boldsymbol{\Psi}^{\prime\prime}\,\mathrm{d}\vec{\rho}^{\,\prime\prime} - \boldsymbol{\Psi}^{\prime}\,\mathrm{d}\vec{\rho}^{\,\prime} = 0,\tag{18}$$

and after division by  $dx'_{k}$ 

$$\Psi''\vec{s}'' = \Psi'\vec{s}'. \tag{19}$$

As  $\vec{s}'$  is known at this point, Eq. (19) constitutes a well-defined system of linear equations for  $\vec{s}''$ .

## 2.2. Special case: infinite dilution

If one of the concentrations, for instance  $\rho_i$ , is zero, the main diagonal element of the Hessian  $\Psi_{ii}$  diverges because of the  $\ln \rho_i$  term in the Helmholtz energy density  $\Psi(\vec{\rho},T)$ . This is the case when, for example, a phase envelope calculation for a ternary mixture is started at a binary phase equilibrium.

As already explained elsewhere [5], this problem can be solved by (a) multiplying Eq. (19) from the left-hand side with a diagonal matrix built from a concentration vector,

$$(\operatorname{diag} \vec{\rho}' \Psi'') \vec{s}'' = (\operatorname{diag} \vec{\rho}' \Psi') \vec{s}', \tag{20}$$

and (b) replacing all  $\Psi_{ii}\rho_i$  terms in Eqs. (16) and (20) by the proper limiting values.

liming varies,
$$\lim_{\rho'_{i}\to 0} \Psi'_{ii}\rho'_{i} = \lim_{\rho''_{i}\to 0} \Psi''_{ii}\rho''_{i} = RT$$

$$\lim_{\rho'_{i}\to 0} \Psi'_{ii}\rho''_{i} = RT\phi_{i}$$

$$\lim_{\rho''_{i}\to 0} \Psi''_{ii}\rho'_{i} = RT\phi_{i}^{-1}$$
with  $\phi_{i} \equiv \exp\left(-\frac{\mu_{i}^{r}'' - \mu_{i}^{r}'}{RT}\right)$ . (21)

The  $\mu_i^{r_\chi}$  are residual chemical potentials of component i, which are well-defined and computable even if some concentrations are zero.

Eqs. (16) and (20) together provide the derivatives that have to be integrated in order to determine the phase envelopes.

## 2.3. Special case: critical states

At a critical point the concentrations  $\vec{\rho}'$  and  $\vec{\rho}''$  become equal. Consequently the system matrix in Eq. (16) has two identical rows, and the equation cannot be solved any longer.

As a workaround we replace the first row of Eq. (16) with an equation for  $s'_{\iota}$ ,

$$\begin{pmatrix}
0 & \dots & 0 & 1 & 0 & \dots & 0 \\
\vec{\Psi}_{1}^{c} \cdot \vec{\rho}^{c} & \dots & \vec{\Psi}_{k-1}^{c} \cdot \vec{\rho}^{c} & \vec{\Psi}_{k}^{c} \cdot \vec{\rho}^{c} & \vec{\Psi}_{k+1}^{c} \cdot \vec{\rho}^{c} & \dots & \vec{\Psi}_{N}^{c} \cdot \vec{\rho}^{c} \\
-x'_{k} & \dots & -x'_{k} & 1-x'_{k} & -x'_{k} & \dots & -x'_{k} \\
a_{l1} & \dots & a_{lk-1} & a_{lk} & a_{lk+1} & \dots & a_{lN} \\
\vdots & \vdots & \vdots & \vdots & \vdots & \ddots & \vdots \\
\vec{s}_{k}^{c} = \begin{pmatrix} f \rho_{k}^{c} \\ 0 \\ \rho^{c} \\ 0 \\ \vdots \end{pmatrix},$$
(22)

where f is a yet unknown scalar.

In the vicinity of a critical point the vector connecting the two coexisting phases,  $\vec{\rho}'' - \vec{\rho}'$ , is approximately aligned with the critical eigenvector  $\vec{u}_1^c$ , i.e., with the eigenvector of  $\Psi^c$  that is associated with  $\lambda_1$ , the lowermost eigenvalue,

$$(\vec{\rho}'' - \vec{\rho}') \propto \vec{u}_1^{c}. \tag{23}$$

The alignment is not exact, since a step along the eigenvector,  $\vec{\rho}^c \rightarrow \vec{\rho}^c + \alpha \vec{u}_1^c$ , is usually neither an isobaric process nor in accordance with the constraints. In most cases, however, the alignment is good enough to obtain approximations for the derivative vectors:

(a)  $\vec{s}'$  is obtained as solution of Eq. (22) while varying f until the condition

$$\frac{\vec{s}' \cdot \vec{u}_1^c}{|\vec{s}'|} \to \text{max with } |\vec{s}'| \equiv \sqrt{\vec{s}' \cdot \vec{s}'}$$
 (24)

is fulfilled.

(b) Then  $\vec{s}''$  is found by following  $\vec{u}_1^c$  into the opposite direction,

$$\vec{s}'' = \vec{s}' - \frac{\vec{s}' \cdot \vec{u}_1^c}{|\vec{s}'|} \vec{u}_1^c, \tag{25}$$

assuming that  $\vec{u}_1^c$  is normalized.

The slope vectors can be used *in principle* to initialize a phase envelope calculation at a critical point of a mixture. As will be explained in the next section, however, there are practical reasons why this approach often fails, particularly for mixtures with more than three components.

## 3. Application

The integration can be conveniently performed with a variety of standard methods, e.g., the Runge–Kutta–Fehlberg method [12] or the Cash–Karp method [13].

The elements of the Hessian matrices  $\Psi'$  and  $\Psi''$  can be obtained directly from the Helmholtz energy density equation by precise (multi)complex numerical differentiation or by automatic formal differentiation [11,14].

It is not necessary to invert the equation of state, i.e., to calculate molar volumes for a given pressure, as the isobaric condition is already contained in the differential equations. This avoids a time-consuming auxiliary calculation.

In order to avoid the accumulation of errors in the course of the integration it is advisable to "polish" the integration results by using them as starting values for an iterative solver of the algebraic equilibrium conditions; usually a single iteration step is sufficient. In the vicinity of critical points, however, more steps may be needed, as here the condition of the linear equations Eqs. (16) and (20) deteriorates. In principle any phase equilibrium algorithm for multicomponent mixtures can be used for this. The methods of Quiñones and Deiters [10,11] and of Nichita [15] offer the advantage that they, too, no not require the inversion of the equation of state. For the examples presented below the former method was used.

Table 1
Parameters of the Peng–Robinson equation used in this work.

component	$a_{\rm c}/({\rm J~cm^3~mol^{-2}})$	b/(cm <sup>3</sup> /mol)	ω
methane	$2.49637322 \times 10^{5}$	26.7771081	0.011
ethane	$6.04124604 \times 10^{5}$	40.4800508	0.099
propane	$1.01769308 \times 10^{6}$	56.3124099	0.153
methane-ethane	$2.95008705 \times 10^{5}$	33.6286961	
methane-propane	$4.86444937 \times 10^{5}$	41.5447590	
ethane-propane	$7.80374655 \times 10^{5}$	48.3963469	

In conventional calculations of phase envelopes – by solving algebraic equations – it is a common "trick of the trade" to use polynomial extrapolation of already established equilibrium states to obtain initial values for the next one. This has some superficial similarity to the method proposed here, namely the integration of differential equations. Polynomial extrapolation, however, lacks thermodynamic insight and is usually much less accurate.

The topology of ternary and higher phase diagrams can change very much over small ranges of pressure or temperature. It is therefore advisable to use parametric marching [16] or other techniques that let the phase envelope calculation "go around bends" [15,17,18]. The following Gibbs triangles illustrate this.

We present here some phase diagrams for the ternary system (methane + ethane + propane), computed with the Peng–Robinson equation of state [19] and the usual Soave-style mixing rules. The parameters are listed in Table 1. The diagrams were created with the ThermoC program package [20]. The integration runs were started at the left triangle edge, i.e., at the (methane + propane) phase equilibrium.  $x_2'$  was used as the marching variable; parametric marching was turned on.

At low pressure (2.5 MPa) methane and ethane are both in the vapor state, whereas propane is a liquid. Consequently the phase diagram is of the band type. At 7.4 MPa ethane liquefies, and so the band shifts to the lower edge of the triangle diagram (Fig. 1).

At higher pressures the two-phase region detaches from the lower edge and contracts, until it vanishes in a critical boundary point (Fig. 2).

Fig. 3 illustrates the behavior of the concentrations along the phase boundaries as functions of the marching variable  $(x_2')$ . The inserts are magnifications of the critical region. They show that the slopes  $s_i' = \mathrm{d}\rho_i'/\mathrm{d}x_2'$  and  $s_i'' = \mathrm{d}\rho_i''/\mathrm{d}x_2'$  are almost oppositely equal at the critical point. The arrows in Fig. 3 indicate the predictions from Eqs. (24) and (25).

A peculiar feature is the "hook" that some of the curves exhibit close to the critical point; it underlines the importance of parametric marching or similar algorithms [17,18] when exploring such phase diagrams.

The existence of these "hooks" is one of the reasons why it is difficult to initialize the integration of the concentration derivatives at a critical point: The  $\rho_1^{\chi}(x_2')$  and  $\rho_3^{\chi}(x_2')$  functions are strongly curved and change their slopes rapidly. It is therefore necessary to use a small integration step size. This, however, requires solving Eqs. (16) and (20) so close to the critical point that they are ill-conditioned and their solutions become numerically unstable.

The  $\rho_2^\chi(x_2')$  function in this example seems to be better behaved. However, its limiting slopes can become very large, possibly even infinite, and this would create computational problems, too.

When during a phase envelope calculation an isothermal–isobaric phase envelope of a *ternary* mixture is followed through a critical point, the liquid phase becomes the vapor phase and vice versa. Therefore Figs. 1 and 2 contain single phase envelopes. If there are more then

<sup>&</sup>lt;sup>1</sup> These phase diagrams merely serve to illustrate the topology of phase diagrams. We do not strive to match experimental data nor recommend this equation of state or our parameter set.

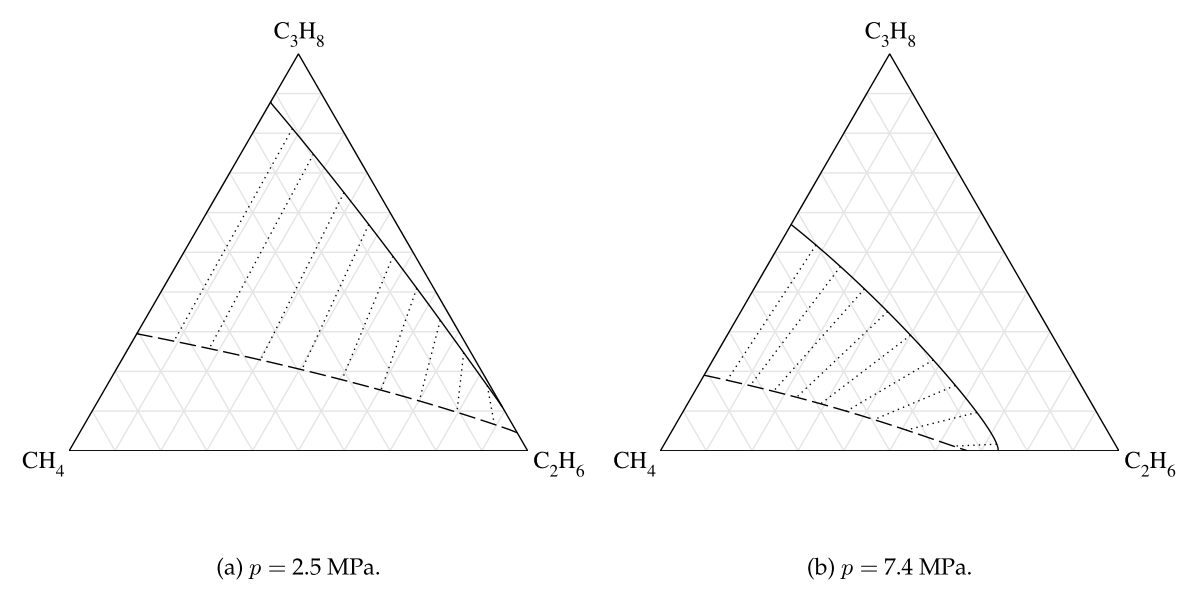


Fig. 1. Gibbs triangle of the (methane + ethane + propane) system at 280 K and (a) 2.5 MPa, (b) 7.4 MPa. —— liquid phase, -- - vapor phase, ...... connodes.

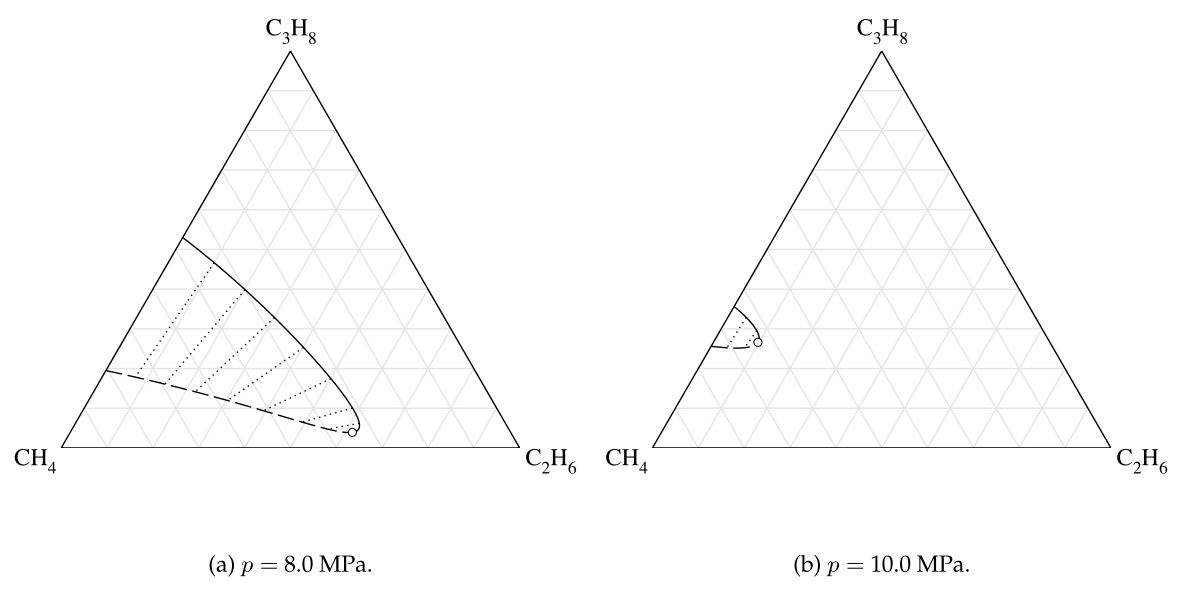


Fig. 2. Gibbs triangle of the (methane + ethane + propane) system at 280 K and (a) 8.0 MPa, (b) 10.0 MPa. —— liquid phase, - - - vapor phase, ... ... connodes, o ternary critical point.

three components, however, it is necessary to specify constraints. These constraints apply to the ' phase, not to the coexisting " phase. When the boundary curve of constrained liquid phase is followed through a critical point, it becomes the boundary curve of a constrained vapor phase—and this is different from the boundary curve of the unconstrained vapor phase. The reverse is true for the coexisting vapor phase. Therefore an isothermal–isobaric phase diagram phase diagram of a mixture of four or more components contains two sets of phase boundary curves, which intersect in the critical point.

This is illustrated by Fig. 4, which shows the  $x_2^{\chi}$  vs.  $x_1^{\chi}$  phase diagram<sup>2</sup> of the 5-component mixture (methane + butane + heptane

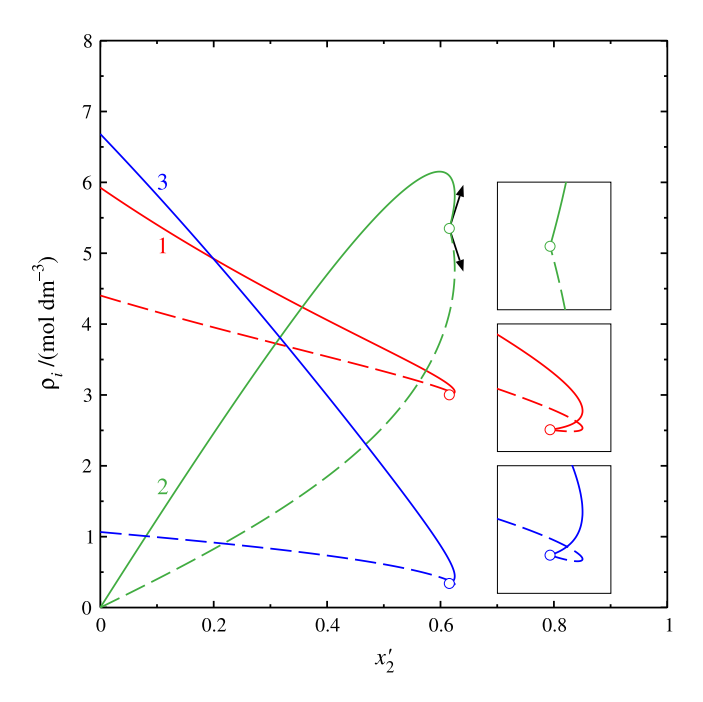
+ decane + tetradecane) at 529.51 K and 13.94 MPa, computed again with the Peng–Robinson equation of state. For this calculation all  $k_{ij}$  factors were set to 0. The constraints were  $x_4'/x_3'=0.5$  and  $x_5'/x_3'=1$ . The marching mole fraction was  $x_1'$ .

Fig. 5 shows the concentrations of the five components as functions of the marching mole fraction  $x'_1$ . The arrows indicate the predicted directions of the derivative vectors for Component 1 (methane) at the critical point. Again the curves exhibit sharp "hooks" that require advanced marching methods.

## 4. Conclusion

The algorithm for isothermal-isobaric phase envelopes proposed here is based on the integration of ordinary differential equations.

<sup>&</sup>lt;sup>2</sup> We refrain from displaying a 4-dimensional Gibbs hypertetrahedron.



**Fig. 3.** Concentrations (molar densities)  $\rho_1^\chi$  (red),  $\rho_2^\chi$  (green), and  $\rho_3^\chi$  (blue) as functions of the marching variable  $x_2'$  for the phase diagram Fig. 2a. —— liquid phase, – – vapor phase,  $\circ$  ternary critical point.

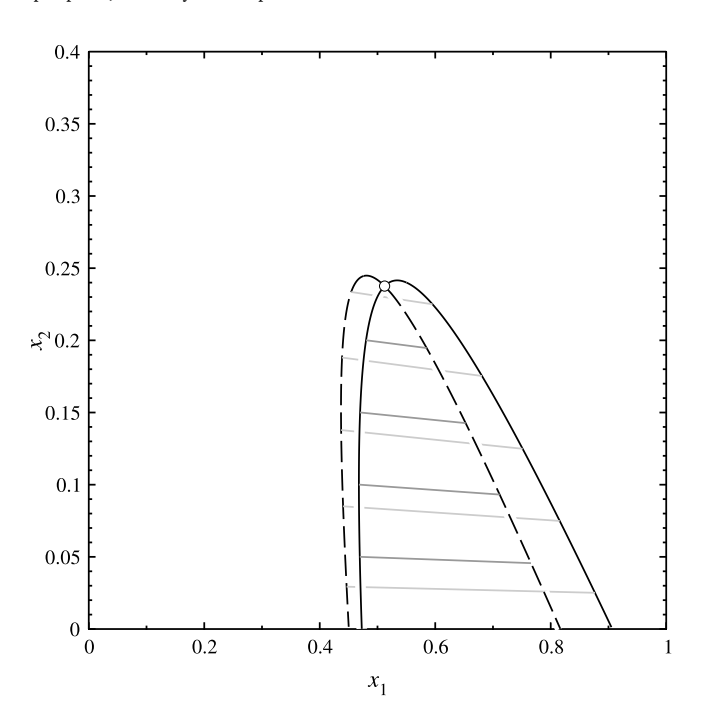


**Fig. 4.** Vapor–liquid equilibrium of (methane + butane + heptane + decane + tetradecane) at 529.51 K and 13.94 MPa, computed with the Peng–Robinson equation of state:  $x_2^\chi$  vs.  $x_1^\chi$ . Black curves: — constrained phase, – – unconstrained phase; gray lines: connodes,  $\circ$  quinary critical point.

It avoids the convergence problems that so often hamper algorithms based on the numerical, iterative solution of the algebraic equations describing phase equilibria. The time-consuming calculation of densities for the given pressure is never required. The new algorithm is very rapid, and it is particularly useful for thermodynamic models that can return physically unreasonable results for some combinations of their state variables.

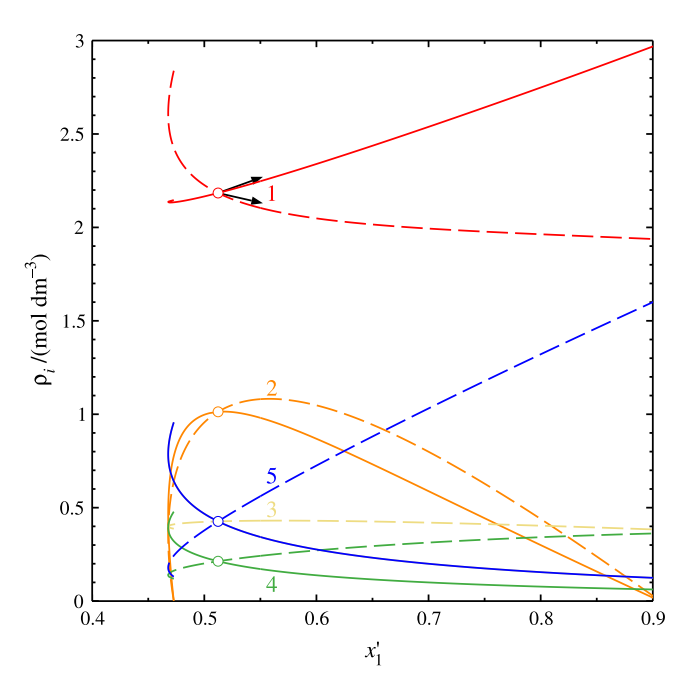


**Fig. 5.** Concentrations (molar densities)  $\rho_i^{\gamma}$ ,  $i=(1,\ldots,5)$  (colors red, ..., blue) as functions of the marching variable  $x_1'$  for the 5-component system of Fig. 4. — constrained phase, – – unconstrained phase,  $\circ$  quinary critical point. The solid curve of Component 3 lies under the curve of Component 5.

# **Symbols**

$a_{li}$	constraint coefficient of component <i>i</i> in the /th
	constraint
$\vec{a}_l$	vector of coefficients of the <i>l</i> th constraint,
	$\vec{a}_l \equiv (a_{l1}, \dots, a_{lN})$
N	number of components
p	pressure
$\vec{s}$ $\chi$	derivative vector, $\vec{s}^{\chi} \equiv (s_1^{\chi}, \dots, s_N^{\chi})$ with $s_i^{\chi} \equiv d\rho_i^{\chi}/dx_k' _{\sigma}$
T	temperature
$\vec{u}_1$	eigenvector associated with the lowermost eigenvalue
	of $oldsymbol{arPsi}$
$x_i$	mole fraction of component i
$\mu_i^{ m r} \ ec{\mu}$	residual chemical potential of component i
$\vec{\mu}$	vector of chemical potentials, $\vec{\mu} \equiv (\mu_1, \dots, \mu_N)$
ρ	molar density, $\rho \equiv V_{\rm m}^{-1}$
$ ho_i$	concentration (molar density) of component i
$\vec{ ho}$	vector of concentrations, $\vec{\rho} \equiv (\rho_1, \dots, \rho_N)$
Ψ	Helmholtz energy density, $\Psi \equiv A/V$
Ψ	Hessian matrix of $\Psi$
$ec{oldsymbol{\Psi}}_i$	<i>i</i> th row vector of $\Psi$
$\Psi_{ii}$	matrix element of $\Psi$

## **Declaration of competing interest**

The authors declare that they have no known competing financial interests or personal relationships that could have appeared to influence the work reported in this paper.

# Acknowledgments

The author thanks Ian H. Bell, NIST, Boulder (Colorado), USA and Sven Pohl, Ruhr University, Bochum, Germany, for proposing this study.

#### Data availability

Data will be made available on request.

### References

- M.L. Michelsen, Calculation of phase envelopes and critical points for multicomponent mixtures, Fluid Phase Equilib. 4 (1980) 1–10, http://dx.doi.org/10.1016/ 0378-3812(80)80001-X
- [2] O. Kunz, W. Wagner, The GERG-2008 wide-range equation of state for natural gases and other mixtures: an expansion of GERG-2004, J. Chem. Eng. Data 57 (2012) 3032–3091, http://dx.doi.org/10.1021/je300655b.
- [3] D. Konowalow, Über die Dampfspannungen der Flüssigkeitsgemische, Ann. Phys. 250 (1881) 34–52, 219–226, volume also cited as Wied. Ann. 14.
- [4] R. Haase, Thermodynamik der Mischphasen, Springer, Berlin, 1956.
- [5] U.K. Deiters, Differential equations for the calculation of fluid phase equilibria, Fluid Phase Equilib. 428 (2016) 164–173, http://dx.doi.org/10.1016/j.fluid. 2016.04.014.
- [6] U.K. Deiters, Differential equations for the calculation of isopleths of multicomponent fluid mixtures, Fluid Phase Equilib. 447 (2017) 72–83, http://dx.doi.org/ 10.1016/j.fluid.2017.03.022.
- [7] U.K. Deiters, I.H. Bell, Differential equations for critical curves of fluid mixtures, Ind. Eng. Chem. Res. 59 (2020) 19061–19076, http://dx.doi.org/10.1021/acs. iecr.0c03667.
- [8] I.H. Bell, U.K. Deiters, On the construction of binary mixture p-x and T-x diagrams from isochoric thermodynamics, AIChE J. 64 (2018) 2745–2757, http://dx.doi.org/10.1002/aic.16074.

- [9] U.K. Deiters, I.H. Bell, Unphysical critical curves of binary mixtures predicted with GERG models, Int. J. Thermophys. 41 (2020) 169, http://dx.doi.org/10. 1007/s10765-020-02743-3, 1-19.
- [10] S.E. Quiñones-Cisneros, U.K. Deiters, An efficient algorithm for the calculation of phase envelopes of fluid mixtures, Fluid Phase Equilib. 329 (2012) 22–31, http://dx.doi.org/10.1016/j.fluid.2012.05.023.
- [11] U.K. Deiters, T. Kraska, in: E. Kiran (Ed.), High-Pressure Fluid Phase Equilibria— Phenomenology and Computation, second ed., in: Supercritical Fluid Science and Technology, vol. 2, Elsevier, Amsterdam, 2023.
- [12] Runge-Kutta-Fehlberg method (RK45), 2025, https://en.wikipedia.org/wiki/ Runge-Kutta-Fehlberg method, (Accessed 22 February 2025).
- [13] J.R. Cash, A.H. Karp, A variable-order Runge–Kutta method for initial-value problems with rapidly varying right-hand sides, ACM Trans. Math. Software 16 (1990) 201–222, http://dx.doi.org/10.1145/79505.79507.
- [14] I.H. Bell, U.K. Deiters, A.M.M. Leal, Implementing an equation of state without derivatives: teqp, Ind. Eng. Chem. Res. 61 (2022) 6010–6027, http://dx.doi.org/ 10.1021/acs.iecr.2c00237.
- [15] D.V. Nichita, Density-based phase envelope construction, Fluid Phase Equilib. 478 (2018) 100–113, http://dx.doi.org/10.1016/j.fluid.2018.09.007.
- [16] U.K. Deiters, I.H. Bell, Calculations of phase envelopes of fluid mixtures through parametric marching, AIChE J. 65 (2019) e16730, http://dx.doi.org/10.1002/ aic.16730, 1–13.
- [17] G. Venkatarathnam, Density marching method for calculating phase envelopes, Ind. Eng. Chem. Res. 53 (2014) 3723–3730, http://dx.doi.org/10.1021/ie403633d.
- [18] I.K. Nikolaidis, I.G. Economou, G.C. Boulougouris, L.D. Peristeras, Calculation of the phase envelope of multicomponent mixtures with the bead spring method, AIChE J. 62 (2016) 868–879, http://dx.doi.org/10.1002/aic.15064.
- [19] D.Y. Peng, D.B. Robinson, A new two-constant equation of state, Ind. Eng. Chem. Fundam. 15 (1976) 59–64, http://dx.doi.org/10.1021/i160057a011.
- [20] U.K. Deiters, ThermoC project homepage, 2025, http://thermoc.uni-koeln.de/ index.html, (Accessed 21 January 2025).